Chapter 12

Grain and Pore Structure Imaging of Gas Hydrate From Core MD02-2569 (Mississippi Canyon, Gulf of Mexico): A First Look by Scanning Electron Microscopy (SEM)

Laura A. Stern[1] and Stephen H. Kirby[1]

Grain and pore structure imaging of gas hydrate from core MD02-2569 (Mississippi Canyon, Gulf of Mexico): A first look by Scanning Electron Microscopy (SEM); chapter 12 in *Winters, W.J., Lorenson, T.D., and Paull, C.K., eds., 2007, Initial report of the IMAGES VIII/PAGE 127 gas hydrate and paleoclimate cruise on the RV* Marion Dufresne *in the Gulf of Mexico, 2–18 July 2002: U.S. Geological Survey Open-File Report 2004–1358.*

Abstract

Natural gas hydrate nodules from core MD02-2569, Gulf of Mexico/Mississippi Canyon site, were imaged by Scanning Electron Microscopy and compared to similar features observed in lab-synthesized gas hydrates of known composition, grain texture, and pressure-temperature histories.

Introduction

One of the challenges of investigating both natural and laboratory-made gas hydrates involves evaluation of their grain and pore structures, characteristics that are revealing guides to the physics and chemistry of hydrate formation, and the effects of changes in environmental conditions. Such structural and textural details also influence the specific effects of gas hydrates on sediment properties.

Scanning Electron Microscopy (SEM) offers significant potential for obtaining such textural information because of its versatility in detection capabilities, its resolution, and its large depth of focus. When applied to gas hydrates, however, numerous technical challenges must be considered: avoiding condensation of atmospheric water on samples during cold transfer, coating samples with an electrically conductive layer without introducing heat or damage to the sample surface, maintaining the hydrate sample material at conditions that avoid spontaneous decomposition or substantial sublimation under vacuum, and either avoiding electron beam damage of the imaging area or properly identifying it when it occurs. Distinguishing handling-induced surface artifacts from the intrinsic sample surface morphology also can be difficult, as well as distinguishing hydrate from water ice. Few SEM images of gas hydrates have been published; work by Kuhs and his coworkers being notable exceptions (Kuhs and others, 2000; Techmer and others, 2001, 2005; Suess and others, 2002; Klapproth and others, 2003; Staykova and others, 2003; Genov and others, 2004), as well as work from our own laboratory (Stern and others, 2002, 2003, 2004; Circone and others, 2003; Stern, Circone, and others, 2005; Stern, Kirby, and others, 2005).

For the study of natural (as opposed to lab-synthesized) gas hydrates, these challenges are greatly amplified by such additional unknowns as the complex in situ environmental conditions controlling the original growth textures or the effects of subsequent recrystallization, annealing, secondary growth, dissociation, dissolution, or chemical exchange processes. The indeterminate extent of sample damage or alteration incurred during retrieval and subsequent storage or handling of the hydrate presents additional unknowns. Without a wider sampling archive and additional experience with assessing these issues, most interpretations of SEM images of natural gas hydrates, therefore, should be regarded as speculative. Nonetheless, useful information about grain structure, pore characteristics, phase composition, and phase distribution may still be gleaned from even preliminary work, particularly if the natural hydrates can be compared to other materials with well-known histories, including lab-synthesized samples.

Here, we present a suite of images offering a “first look” at some natural gas hydrate nodules recovered from research

[1]U.S. Geological Survey, Menlo Park, CA 94025 USA.

vessel (RV) *Marion Dufresne* core MD02-2569 (Mississippi Canyon, Gulf of Mexico), and compare the observed features to those previously documented (Stern and others, 2002, 2003, 2004) in lab-synthesized gas hydrates of known composition, grain structure, and pressure-temperature processing histories. These results are purely qualitative, as we are unable to obtain direct compositional information on the MD02 hydrates at this time. We offer preliminary interpretations drawn from comparison with our SEM image archive of a wide variety of other gas hydrate samples, including pure end-member gas hydrates grown in our laboratory, samples used in compaction and deformation experiments, samples from dissolution experiments, samples of varying (and known) porosity, samples with known fractions of ice and hydrate, and samples used in surface sublimation or partial decomposition tests to help distinguish hydrate from ice.

Experimental Methods

The RV *Marion Dufresne* samples were sent by air freight from St. Petersburg, FL, to the USGS in Menlo Park, CA, in liquid-nitrogen-cooled "dry shippers" approximately 2 months after sample recovery. Upon arrival, the samples were transferred to deep-freezer storage at –90 degrees Celsius (°C). The bulk samples included fine-grained white nodules that were sometimes surrounded by translucent ice or sometimes interspersed with fine-grained sediments. Several samples arrived in small pieces. The white material from both the nodules and fragments actively degassed when warmed and appeared to be composed primarily of hydrate. Information on gas hydrate specimens present in the Gulf of Mexico can be found in Lorenson and others (this volume, chapters 2 and 9) and Winters and others (this volume, chapter 3). Prior to SEM imaging, each sample was immersed in liquid nitrogen while a small section of hydrate, typically 0.75 x 0.75 x 0.5 centimeter (cm), was cleaved for imaging. The section was then attached to a specially designed sample holder.

Surfaces of the sections were prepared and imaged with a LEO 982 field emission SEM equipped with a Gatan Alto 2100 cryo-preparation and coating station, and cryo-imaging stage. The samples, initially in liquid nitrogen, were quickly transferred to the evacuated and pre-chilled (to below –178 °C) preparation chamber, then fractured by cold blade to produce fresh surfaces for viewing. While still in the preparation chamber, the samples were coated with AuPd using a non-heat-emitting sputter head. Samples were then inserted directly through the back of the preparation chamber onto the auxiliary cryo-imaging stage in the SEM column. Imaging was conducted at temperatures below –168 °C and vacuum below 10^{-5} millibar (mbar), using low voltage ($\leq$2 kilovolt (kV)) to minimize sample alteration or beam damage of the sample surface. Several imaged areas were re-examined later in the session to monitor vacuum effects or changes in surface topology over time, a procedure routinely used during SEM imaging of any hydrate- or ice-bearing materials (see Stern and others, 2004, for further technical description of SEM procedures). A companion sample of methane hydrate was also imaged uncoated to ensure that surface topology was not altered by the coating process. Upon subsequent removal from the SEM, all samples actively degassed upon warming, as evidenced by vigorous bubble formation on the specimen surfaces.

Phase identification was not part of this imaging study because our SEM port requirements necessitate removal of the back-scattered electron detector when the cryosystem is in use. Use of energy dispersive x-ray (EDX) capabilities also was problematic because of the long focal distance needed for that technique combined with the low accelerating voltage needed to ensure minimal damage of hydrate. While EDX detection of carbon can permit distinction of hydrocarbon hydrates from ice in some cases where the hydrate has nearly complete guest-molecule site occupancy (Stern and others, 2004; Stern, Kirby, and others, 2005), this method did not yield convincing results on the partially decomposed MD02 samples.

Results and Discussion

Figures 1 and 2 show low-to-high resolution mosaics of the interiors of hydrate nodules from core MD02-2569, and figure 3 shows characteristic textures from near the outer surface and from the mixed hydrate + sediment ± ice sections. Interpretation of the images remains somewhat uncertain given the many unknowns involving bulk sample composition, phase distribution, partial alteration of original textures and(or) composition during the recovery process, and other factors already discussed above. These mosaics, therefore, are presented primarily to give the reader a general sense of the appearance of the as-received sample texture, pore structure, and pore connectivity.

Without more information for definitive interpretation, our best option is to compare the imaged textures with those of known materials having well-characterized composition, grain structure, and known pressure-temperature histories. Figure 4 shows both low- and high-resolution features from the natural hydrate (left column) compared to those of pure methane hydrate used in partial dissolution and(or) dissociation experiments (right column). The samples shown in the right column initially were synthesized in our laboratory by previously published methods (Stern and others, 1996, 2000) that produce pure methane hydrate of composition $CH_4 \cdot 5.9H_2O$. Two samples were compacted hydrostatically (while maintained within their equilibrium stability field) from 30-percent to less than 3-percent porosity, then transported under pressure to an ocean floor test site at 1,030-meter (m) water depth for observation and measurement (see Stern and others, 2003, and Rehder and others, 2004, for further details). Two samples of uncompacted methane hydrate were also sent down in the experiment. Those samples that did not fully dissolve after 26 hours were successfully retrieved for SEM imaging (fig. 4B, D, F, and H).

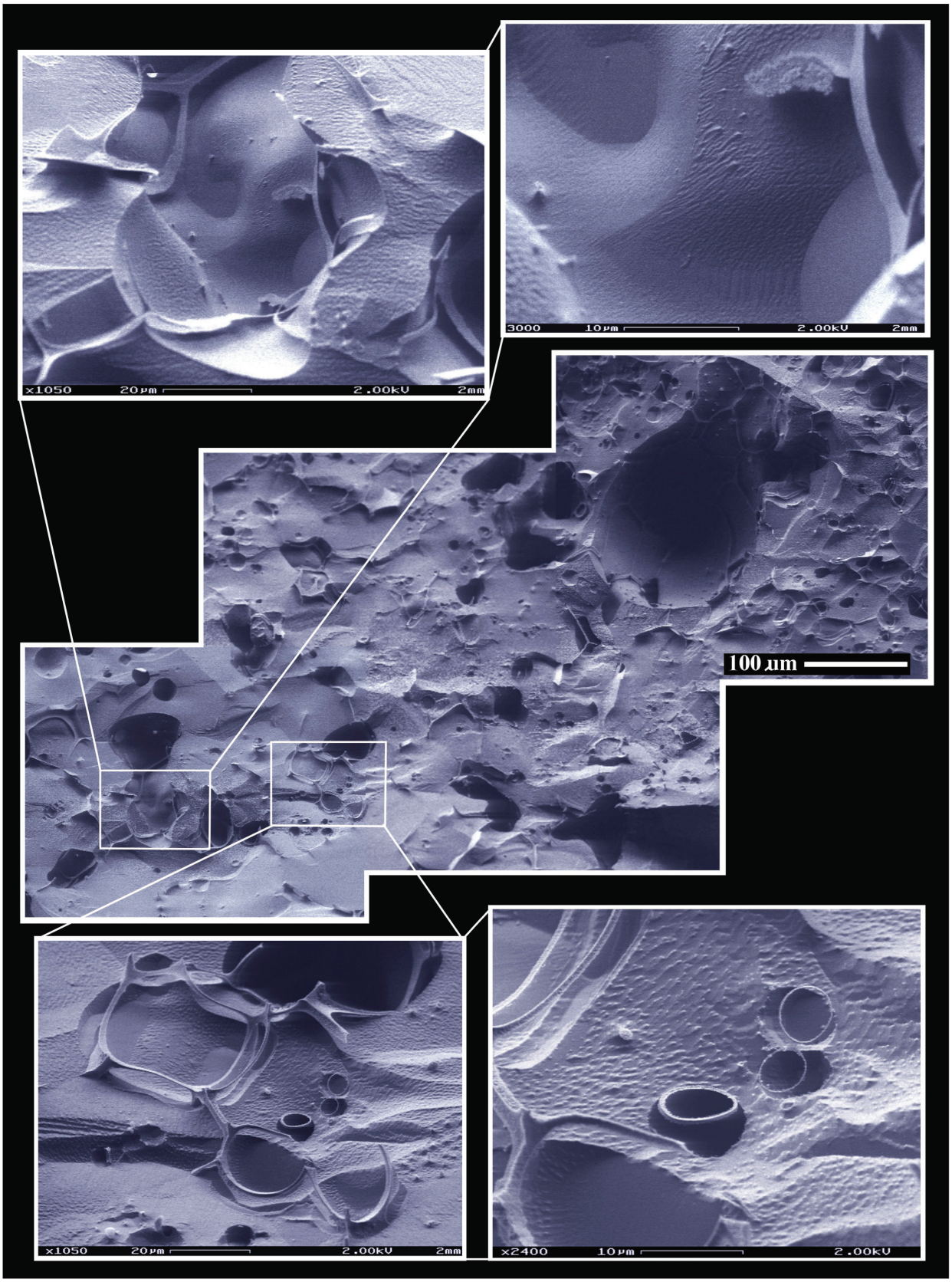

Figure 1. Scanning Electron Microscopy (SEM) mosaic showing a typical section within a gas hydrate "nodule" from core MD02-2569.

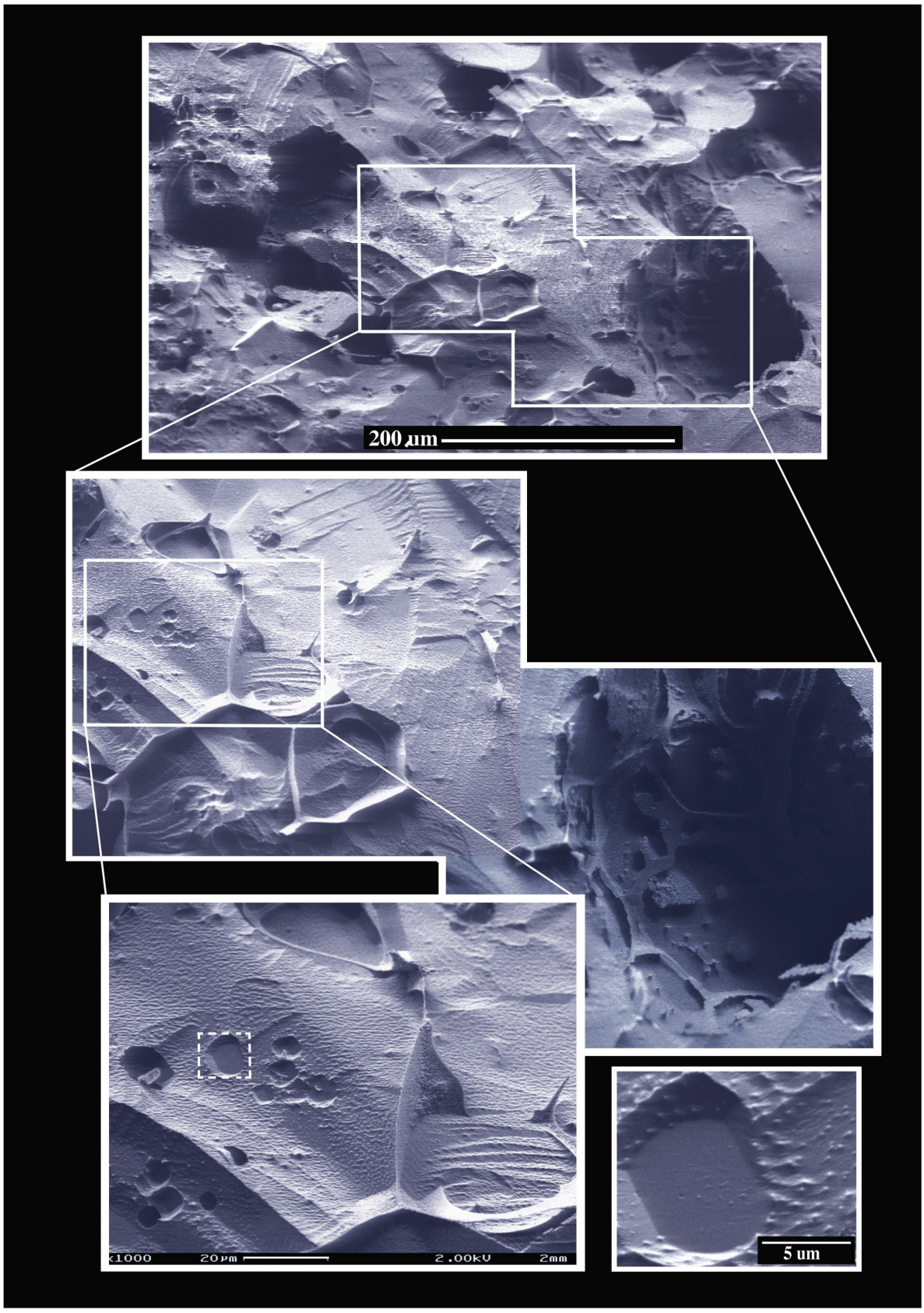

Figure 2. Low-to-high resolution Scanning Electron Microscopy (SEM) mosaic showing textural features within a second subsection of the gas hydrate nodule shown in figure 1.

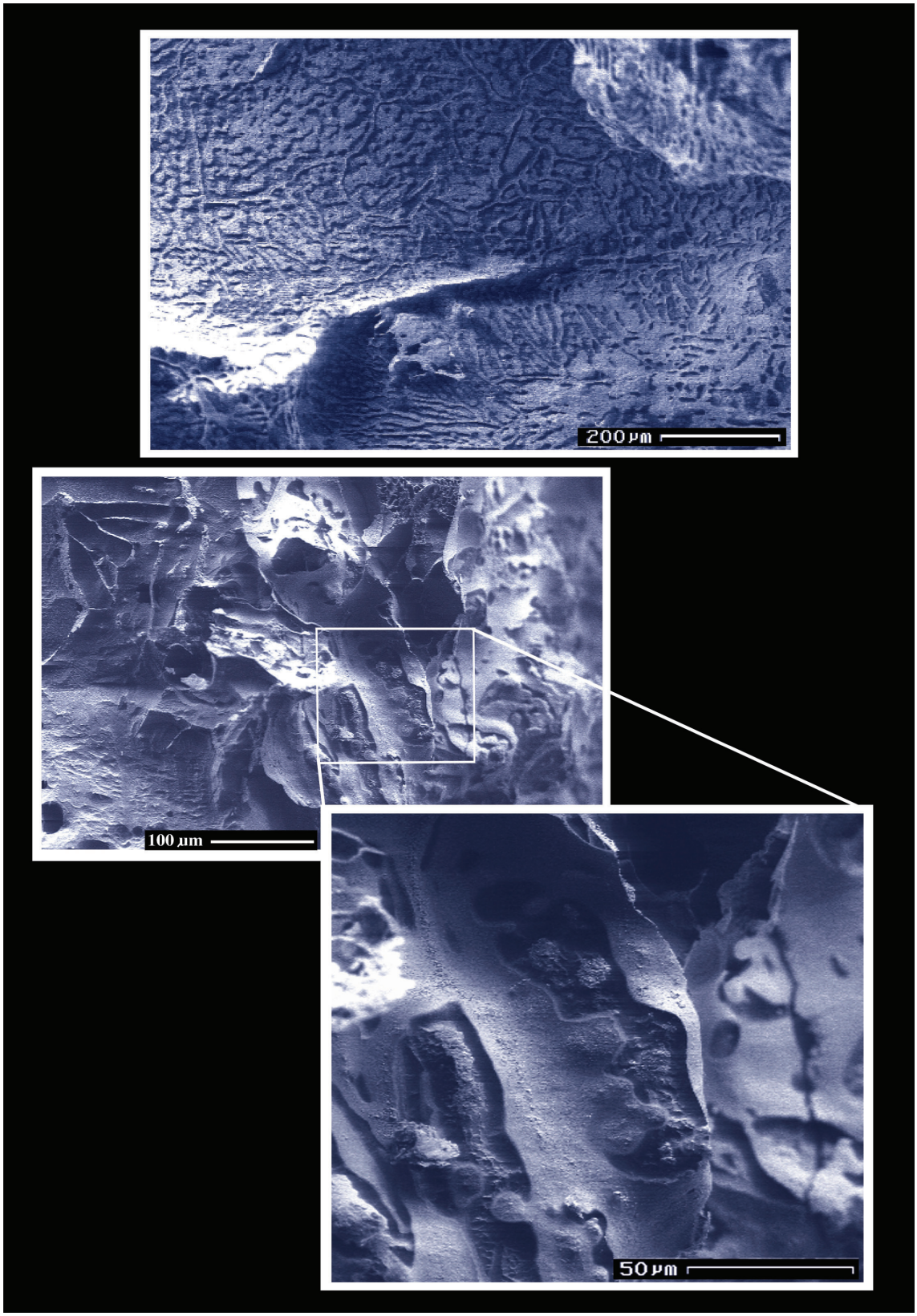

Figure 3. Images from a near-surface section from core MD02-2569 (top photograph) showing what may be partial dissolution textures (compare with figure 4B) and a section through the hydrate/sediment portion of the sample (lower two photographs).

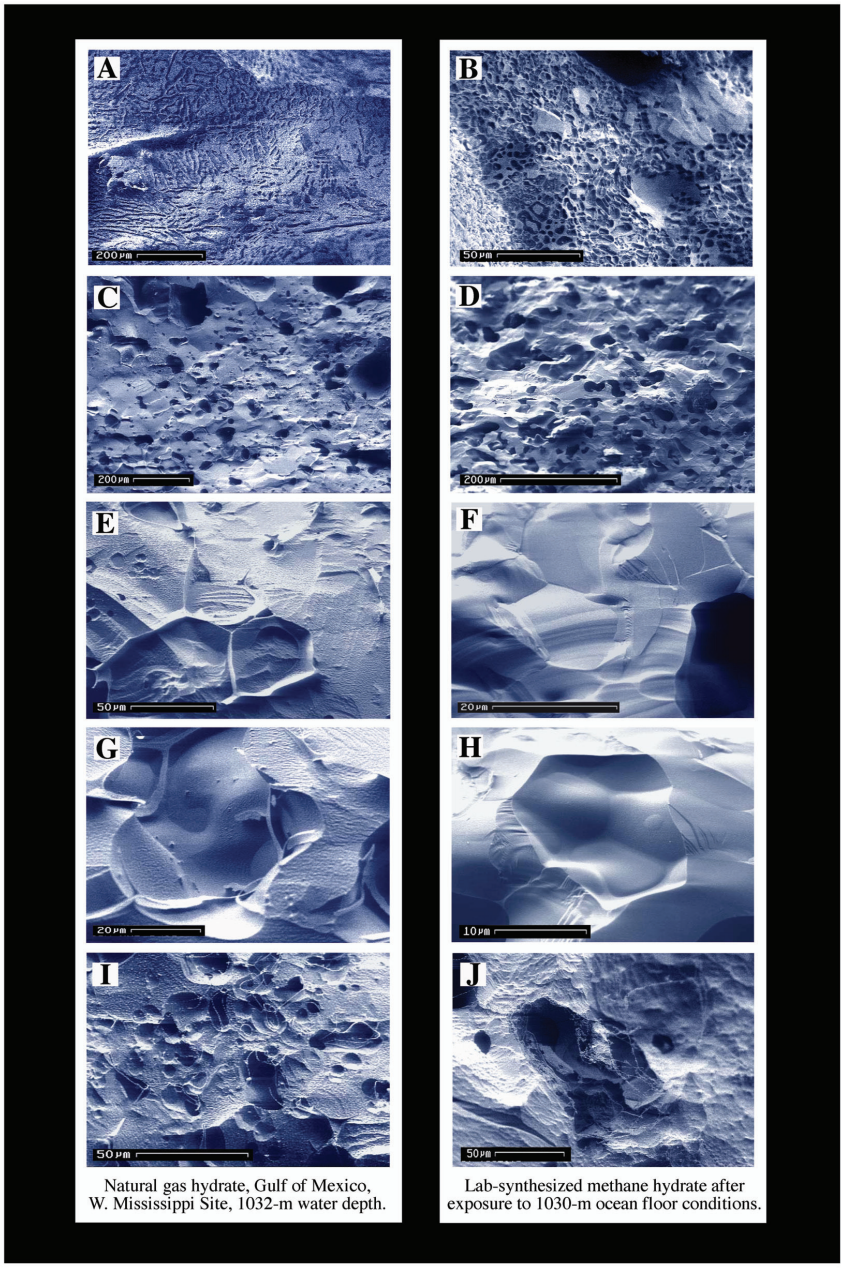

Figure 4. Comparison of Gulf hydrate (left column) to lab-synthesized methane hydrate used in partial dissolution or dissociation experiments (right column). A and B show similarities in grain boundary and pore "cast" textures. A is from a near-surface section of the natural hydrate, and B is a 30-percent porous methane hydrate sample that underwent partial dissolution before subsequent retrieval (see text for further discussion). C and D show similar cavity size, distribution, and cavity connectivity in partially compacted sections of samples. The lab-synthesized sample shown in D was compacted to < 3-percent porosity, although the remaining porosity is not homogeneously distributed throughout the sample. E and F show similarities in grain size, material "density," and clean fracture surfaces. Neither the natural or lab-synthesized material appears to be mesoporous, in contrast with some synthetic and natural methane hydrates discussed in Kuhs and others (2000), Techmer and others (2001), and Suess and others (2002). See also Stern and others (2004, 2005a, 2005b) for further discussion of porous microstructural development. The grain size of the pure methane hydrate sample shown in F is several 10's of microns, which is typical of our synthetic hydrate despite growth conditions from initially larger (~200 micrometers (µm)) ice grains. G and H show minimal-surface-area grain textures along cavity walls that we interpret (based on comparison to features observed in low temperature experiments) as grain growth or annealing at the relatively warm conditions (above 0 degrees Celsius) of marine environments. I and J show similar "frothy" or sponge-like textural development indicative either of partial dissociation of gas hydrate to ice, or to hydrate dissociation to water followed by rapid quenching in liquid nitrogen. The sample shown in J was used in controlled low-temperature (< 0 degrees Celsius) partial dissociation experiment discussed more fully in Stern and others (2003), and its surface is known to be composed of both hydrate and the dissociated ice product.

The test site essentially was the same depth from which core MD02-2569 samples were retrieved, hence offering a basis for comparison.

Despite the relatively short duration of the ocean-floor experiment, the interiors of both the compacted and uncompacted hydrates showed surprisingly different grain and pore structure than the original densely crystalline material (compare to figs. 6, 7, and 10 in Stern and others, 2004, for example). Even more surprising was the striking similarity in textural and structural development displayed by core MD02-2569 material compared with the synthetic samples. For instance, the highly faceted and finely crystalline grain morphology pervasive in many of our as-grown gas hydrate materials (Stern and others 2004, figs. 6, 7, 8) is conspicuously absent from all ocean-floor or sub-ocean-floor samples that we have imaged to date. Instead, those samples exposed to deep marine conditions developed minimal-surface-area grain structures, as shown in figures 1 and 4. Unusual relic grain "skeletal" features also are commonly found lining cavity walls (fig. 2), although we cannot rule out the possibility that some of these features may be artifacts of hydrate breakdown followed by quenching (for instance, as shown in fig. 4I, J). Cavity and(or) pore geometry also tends to be rounder or more regularly shaped in marine samples than in our lab-grown hydrates formed from gas-reaction with ice, and do not appear to be highly connected in the samples imaged here, except for in near-surface sections of the nodules. All seawater-exposed hydrate samples that we have imaged to date exhibit dense hydrate interspersed with micro- to macro-sized pores, with no observed mesoporosity at the intragranular scale. Further comparison is given in the caption for figure 4.

Conclusion

While the results presented here are clearly preliminary, our initial success with gas hydrate imaging by low-temperature SEM persuades us that it will be an extremely useful tool for further resolving the wide range of grain characteristics and microstructures that develop within both natural and lab-made gas hydrates. Such comparisons also should help us decide how accurately we emulate gas hydrates in nature and should greatly aid in the interpretation of physical property measurements made on these materials.

Acknowledgments

Funding was provided by the U.S. Geological Survey (USGS) Gas Hydrate Project and the Methane Hydrate R&D Program of the U.S. Department of Energy, National Energy and Technology Laboratory. Samples from ocean-floor dissolution tests described in the text and shown in figure 4B, D, F, and H were obtained in collaborative work with Monterey Bay Aquarium Research Institute researchers P. Brewer and E. Peltzer. The authors thank W. Waite and R. Kayen of the USGS for helpful reviews of this manuscript, and R. Oscarson, J. Pinkston, S. Circone (all USGS) and W. Durham (Lawrence Livermore National Laboratory) for their technical assistance.

References

Circone, S., Stern, L.A., Kirby, S.H., Durham, W.B., Chakoumakos, B., Rawn, C., Rondinone, A., and Ishii, Y., 2003, CO_2 hydrate—synthesis, composition, dissociation behavior, and a comparison to structure I CH_4 hydrate: Journal of Physical Chemistry B, v. 107, no. 23, p. 5529–5539.

Genov, G., Kuhs, W., Staykova, D., Goreshnik, E., and Salamatin, A., 2004, Experimental studies of the formation of porous gas hydrates: American Mineralogist, v. 89, no. 8–9, p. 1228–1239.

Klapproth, A., Goreshnik, E., Staykova, D., Klein, H., and Kuhs, W., 2003, Structural studies of gas hydrates: Canadian Journal of Physics, v. 81, no. 1–2, p. 503–518.

Kuhs, W., Klapproth, A., Gotthardt, F., Techmer, K., and Heinrichs, T., 2000, The formation of meso- and macroporous gas hydrates: Geophysical Research Letters, v. 27, no. 18, p. 2929–2932.

Rehder, G., Kirby, S.H., Durham, W.B., Stern, L.A., Peltzer, E.T., Pinkston, J., and Brewer, P., 2004, Dissolution rates of pure methane hydrate and carbon dioxide hydrate in undersaturated seawater at 1000 m depth: Geochimica Cosmochimica Acta, v. 68, no. 2, p. 285–292.

Staykova, D., Kuhs, W., Salamatin, A., and Hansen, T., 2003, Formation of porous gas hydrate from ice powders—diffraction experiments and multi-stage model: Journal of Physical Chemistry B, v. 107, p. 10299–10311.

Stern, L.A., Circone, S., Kirby, S.H., and Durham, W.B., 2003, Temperature, pressure, and compositional effects on anomalous or "self" preservation of gas hydrates: Canadian Journal of Physics, v. 81, no. 1–2, p. 271–283.

Stern, L.A., Circone, S., Kirby, S.H., and Durham, W.B., 2004, Application of Scanning Electron Microscopy (SEM) to investigate growth and annealing of gas clathrate hydrates formed from melting ice: American Mineralogist, v. 89, no. 8–9, p. 1162–1175.

Stern, L.A., Circone, S., Kirby, S.H., and Durham, W.B., 2005, SEM imaging of gas hydrate formation processes and growth textures, and comparison to natural hydrates of marine and permafrost origin, Paper 1046, *in* Proceedings of the 5th International Conference on Gas Hydrates, Trondheim, Norway, v. 1, p. 300–309.

Stern, L.A., Kirby, S.H., and Durham, W.B., 1996, Peculiarities of methane clathrate hydrate formation and solid-state deformation, including possible superheating of water ice: Science, v. 273, p. 1843–1848.

Stern, L.A., Kirby, S.H., and Durham, W.B., 2005, SEM imaging of grain structure and phase distribution within hydrate-bearing intervals from JAPEX/JNOC/GSC et al. Mallik 5L-38—What can we learn from comparisons with laboratory-synthesized samples? *in* Dallimore, S.R., and Collett, T.S., eds., Scientific results from the Mallik 2002 gas hydrate production research well program, Mackenzie Delta, Northwest Territories, Canada: Geological Survey of Canada, Bulletin 585.

Stern, L.A., Kirby, S.H., Durham, W.B., Circone, S., and Waite, W., 2000, Synthesis of pure methane hydrate suitable for measurement of physical properties and decomposition behavior, chap. 25, *in* Max, M.D., ed., Natural gas hydrate—in oceanic and polar subaerial environments: Dordrecht, Kluwer publ., p. 323–349.

Stern, L.A., Peltzer, E., Durham, W.B., Kirby, S.H., Brewer, P., Circone, S., and Rehder, G., 2002, Dissolution of hydrocarbon gas hydrates in seawater at 1030 meters; effects of porosity, structure, and compositional variation as determined by high-definition video and SEM imaging: EOS, Transactions of the American Geophysical Union, v. 83, no. 47, Abstract OS21B-0216.

Suess, E., Borhmann, G., Rickert, D., Kuhs, W.F., Torres, M.E., Trehu, A., and Linke, P., 2002, Properties and fabric of near-surface methane hydrates at Hydrate Ridge, Cascadia Margin, *in* Proceedings of the 4th International Conference on Gas Hydrates, Yokohama, Japan, v. 2, p. 740–744.

Techmer, K., Heinrichs, T., and Kuhs, W., 2005, Cryo-electron microscopic studies of structures and composition of Mallik gas-hydrate-bearing samples, *in* Dallimore, S.R., and Collett, T.S., eds., Scientific results from the Mallik 2002 gas hydrate production research well program, Mackenzie Delta, Northwest Territories, Canada: Geological Survey of Canada, Bulletin 585, 12 p.

Techmer, K., Kuhs, W., Heinrichs, T., and Bohrmann, G., 2001, Scanning Electron Microscopic investigations on natural and synthetic gas hydrates—new insights into the formation process: EOS, Transactions of the American Geophysical Union, v. 82, no. 47, Abstract B21D-01.